

Spatiotemporal chaos in Arnold coupled logistic map lattice*

Ying-Qian Zhang, Xing-Yuan Wang¹

Faculty of Electronic Information and Electrical Engineering
Dalian University of Technology
Dalian 116024, China
zhangyq@dlut.edu.cn; wangxy@dlut.edu.cn

Received: 22 October 2012 / **Revised:** 28 April 2013 / **Published online:** 25 September 2013

Abstract. In this paper, we propose a new spatiotemporal dynamics of Arnold coupled logistic map lattice (ACLML). Here, the coupling method between lattices is not a neighborhood coupling but the non-neighborhood of Arnold cat maps. In the proposed system, the criteria such as Kolmogorov–Sinai entropy density and universality, bifurcation diagram, mutual information, space amplitude and space-time diagrams are investigated in this paper. The new features of the proposed system include the lower mutual information between lattices, larger range of parameters for chaotic behaviors, the higher percentage of lattices in chaotic behaviors for most of parameters and less periodic window in bifurcation diagram. These features are more suitable for cryptography. For numerical simulations, we have employed the coupled map lattices system (CML) for comparison. The results indicate that the proposed system has those superior features to the coupled map lattice system (CML). It should be highlighted that the proposed ACLML is a suitable chaotic system for cryptography.

Keywords: chaos, spatiotemporal, Arnold cat map, logistic.

1 Introduction

Nonlinear characteristics in natural systems are responsible for a great variety of possibilities. Spatiotemporal chaos is one of these possibilities [1–16]. Since the coupled map lattices (CML) as a spatiotemporal chaotic system was initially proposed in [9], many researches concentrated on coupled map lattices and obtained mature theory. Khellat et al. [10] investigated a globally nonlocal couple map lattice of spatiotemporal chaos system. Meherzi et al. [11] proposed one-way coupled-map lattices (OCML) of spatiotemporal

*This research is supported by the National Natural Science Foundation of China (Nos. 61173183, 60973152, and 60573172), the Superior University Doctor Subject Special Scientific Research Foundation of China (No. 20070141014), Program for Liaoning Excellent Talents in University (No. LR2012003), the National Natural Science Foundation of Liaoning province (No. 20082165) and the Fundamental Research Funds for the Central Universities (No. DUT12JB06).

¹Corresponding author.

chaos system. Most of the previous spatiotemporal chaos systems are space regular coupling between lattices. Sinha [15] proposed the random coupling of spatiotemporal system which initiated the study of the non-neighborhood coupling in coupled map lattices. Rajesh et al. [14] developed the synchronization in coupled cells with activator-inhibitor pathways. Mondal et al. [12] presented the enhancement spatiotemporal regularity by rapidly switched random links. Jabeen et al. [7] developed the nonuniversal dependence of spatiotemporal regularity on randomness in coupling connections. Poria et al. [13] presented the enhancement of spatiotemporal regularity in an optimal window of random coupling. Chen et al. [3] developed a randomly coupled chaotic map of spatiotemporal chaos system. These studies [3, 7, 12–15] mentioned above, deal with dynamically changing random links for coupling. And these random links achieve the non-neighborhood coupling by employing probability. Therefore, this kind of randomness is irregular in time. Besides the method of the random links for non-neighborhood coupling, we propose nonlinear chaotic map coupling method to achieve the non-neighborhood coupling. This form of coupling connections are static or deterministic unlike the random links in [15], however the coupling connections are unpredictable because of chaos. Moreover, there are still many unknown complicated natural dynamics of nonlinear chaotic map coupling. For example, space-mediated population dynamics [17] contains species interactions between geometrical areas which is a sort of the spatial nonlinear coupling. Therefore, the study of such systems has important significance.

Since spatial nonlinear coupling is common in natural environment as well as neighborhood coupling in previous systems, the motivation of our work in this paper is to discover the new features of spatial nonlinear coupling based spatiotemporal chaotic systems. Compared with the CML system, we employs Arnold cat map here to be the instance of the nonlinear map for lattices coupling in our proposed chaotic system (ACLML).

The significance of work is not only the study of such new spatiotemporal chaotic dynamics, but its new features which are suitable for cryptography. Since Matthews [18] suggested that a one-dimensional chaotic map could be used as one time pad for encrypting messages, the researchers have proposed various encryption algorithms based on the low dimensional chaotic systems [19, 20], hyper-chaotic systems [21, 22] and spatiotemporal chaotic systems [23–27]. Because the advantages of high efficiency and simplicity of low dimensional chaotic systems, some typical low dimensional chaotic maps, such as logistic map, Arnold map and baker map, have been used in encryptions. However, there are well-known weaknesses for the logistic map, such as small key space and weak security. To overcome the drawback, Fridrich [21] proposed an encryption scheme based on a two-dimensional chaotic map. Compared with simple chaotic maps and two-dimensional chaotic maps, spatiotemporal chaos possesses two additional merits for cryptographic purposes. First, observe that due to the finite computing precision, orbits of temporal discrete chaotic systems will eventually become periodic. However, the period of spatiotemporal chaos is found much longer than that of temporal chaotic maps [28] so that the periodicity problem is practically avoided [29]. Second, a spatiotemporal chaotic system is high-dimensional, having a number of positive Lyapunov exponents that guarantee the complex dynamical behavior or high randomness. It is therefore more difficult to predict the time series generated by this kind of chaotic systems. However, the CML

system which is widely used in encryptions [23–26] is not perfect, i.e., periodic windows in its bifurcation diagram is still large and the value of its mutual information is still high in many pairs of lattices of the CML system. The high value of the mutual information in many pairs of lattices may provide opportunities for the adversary's breaking schemes, because the adversary can recover or substitute the random sequences of the lattice in an encryption scheme by that of another lattice. The periodic windows in its bifurcation diagram can reduce the range of the randomness of time series. Besides, the six patterns of the CML system behaviors [8] and its small range of parameters in fully developed turbulence pattern also restraint the current encryptions schemes [23–26] in secret keys design and security of encryptions schemes. To overcome these drawbacks, we propose ACLML system and obtain its new features such as the lower mutual information between lattices, larger range of parameters for chaotic behaviors, the higher percentage of lattices in chaotic behaviors for most of parameters, less periodic window in bifurcation diagrams. These features avoid the drawbacks of the CML system. Therefore, the proposed ACLML system in spatial nonlinear coupling contains superior highlight features for cryptography.

For the study of the new features in the ACLML system, we take the CML system for the comparison. To qualify spatiotemporal chaos, Kaneko [30, 31] proposed the space-amplitude diagrams, space-time diagrams and Lyapunov exponent for measurements of CML system. Shibata et al. [32] developed the Kolmogorov–Sinai entropy and mean Lyapunov exponent for measurements of CML system. Willeboordse et al. [33] proposed bifurcations for spatial chaos. Therefore, we qualify the complexity of both the ACLML system and the CML system by using the Kolmogorov–Sinai entropy density and universality, bifurcation diagrams, the space-amplitude diagrams and space-time diagrams. Additionally, we employ mutual information between lattices to qualify the performance of both systems in cryptography. The numerical simulations show that the features in the ACLML system are superior to the CML system in properties for cryptography.

2 Arnold coupled logistic map lattice

The logistic map was originally proposed by May [34]. It is a first-order difference equation represented by $f(x) = \mu x(1 - x)$. Arnold coupled logistic map lattice (ACLML) that we proposed considers L logistic maps coupled by Arnold cat map as follows:

$$x_{n+1}(i) = (1 - \varepsilon)f[x_n(i)] + \frac{\varepsilon}{2}\{f[x_n(j)] + f[x_n(k)]\}, \quad (1)$$

where i, j, k are the lattices ($1 \leq i, j, k \leq L$), ε is the coupling parameter ($0 \leq \varepsilon \leq 1$), n is the time index ($n = 1, 2, 3, \dots$) and $f(x) = \mu x(1 - x)$, $\mu \in (0, 4]$. The relations of i, j, k are defined by the Arnold cat map [35] described in the following equation:

$$\begin{bmatrix} j \\ k \end{bmatrix} = A \begin{bmatrix} i \\ i \end{bmatrix} \pmod{L} = \begin{bmatrix} 1 & p \\ q & pq + 1 \end{bmatrix} \begin{bmatrix} i \\ i \end{bmatrix} \pmod{L},$$

where p and q are the parameters of cat map.

The CML with neighbor coupling can be defined as [9]

$$x_{n+1}(i) = (1 - \varepsilon)f[x_n(i)] + \frac{\varepsilon}{2}\{f[x_n(i+1)] + f[x_n(i-1)]\}, \quad (2)$$

where ε is the coupling parameter, the mapping function $f(x) = \mu x(1 - x)$, and $\mu \in (0, 4]$.

The difference in equations between ACLML and CML is the variables j and k in Eq. (1) which are instead of $i - 1$ and $i + 1$ in Eq. (2), respectively.

The parameters p and q make ACLML into diverse dynamics systems. When p and q are assigned with fixed values, most of these dynamical systems even hold chaotic features in continuously varying value of μ in logistic map.

3 Lyapunov exponents and Kolmogorov–Sinai entropy

Lyapunov exponents evaluate the divergence of nearby orbits and provide a qualitative view of the dynamical system. Any system holding chaotic behavior is presented at least one positive Lyapunov exponents. In ACLML, the spatiotemporal chaotic system can be expressed by

$$x_{n+1}(i) = g(x_n(i), x_n(j), x_n(k)).$$

The determination of Lyapunov exponents needs to consider the variation of the initial values in lattices. The Jacobian matrix J_n in [32] is calculated in each iteration. Then we define

$$R_n = \prod_{k=1}^n J_k,$$

where n is iterations. Lyapunov exponents are evaluated from the eigenvalue $\sigma(i)$ of R_n as follows [36]:

$$\lambda(i) = \lim_{n \rightarrow \infty} \frac{\log |\sigma(i)|}{n},$$

where $\lambda(i)$ is Lyapunov exponent.

The spatiotemporal chaotic system of the ACLML can be considered as L dimensions dynamics, the Kolmogorov–Sinai entropy of the L dimensions dynamics is the sum of positive Lyapunov exponents. Without loss of generality, the Kolmogorov–Sinai entropy density is employed here to eliminate the effect of number of lattices, which is presented as follows:

$$h = \frac{\sum_{i=1}^L \lambda^+(i)}{L},$$

where $\sum_{i=1}^L \lambda^+(i)$ is the sum of positive Lyapunov exponents of L lattices.

Hence, when Kolmogorov–Sinai entropy density h is zero, there is no positive Lyapunov exponent which indicates the spatiotemporal chaotic dynamics is in regular behavior. On the other hand, the positive value of Kolmogorov–Sinai entropy density presents the system in chaos.

The Kolmogorov–Sinai entropy density indicates whether the spatiotemporal chaotic system is in chaos. However, Kolmogorov–Sinai entropy density can not present chaotic majority of L lattices since Kolmogorov–Sinai entropy density is positive. Here, we employed Kolmogorov–Sinai entropy universality hu as follows:

$$hu = \frac{L'}{L},$$

where L' is the number of positive Lyapunov exponents in spatiotemporal chaotic system of ACLML. The Kolmogorov–Sinai entropy universality is the percentage of lattices in chaos which evaluates the space complexity in L dimensions of dynamics.

4 New features of ACLML system in dynamical behaviors

For comparison purposes, we focus on the system of the ACLML system by assuming a grid of $L = 100$ as the CML system [8] assigned the same value $L = 100$. The values of parameters p and q should make the Arnold cat map [35] in chaos. Without loss of generality, we assign parameters $p = 12$ and $q = 7$ to explain the features of the proposed system in this section. All simulations are conducted assuming that parameter $\varepsilon \in [0, 1]$ and parameter $\mu \in [3.0, 4.0]$. Those choices of parameters ε, p, q represent different kinds of couplings. The Kolmogorov–Sinai entropy density and universality are calculated from converged Lyapunov exponents. Bifurcation diagrams, space-amplitude diagrams and space-time diagrams are analyzed in this section comparing with the CML system. Mutual information between lattices is also calculated here which indicates non-synchronization in time series between lattices. The initial values of lattices are also concerned above. The idea is to investigate new features that can be adopted in cryptography.

4.1 Kolmogorov–Sinai entropy density and universality in the ACLML system

The analysis of Kolmogorov–Sinai entropy density for different parameter values allows us to identify distinct behavior, as shown in Fig. 1. Flat regions of the system presents chaotic behaviors when $\mu > 3.63$ and $\varepsilon \in (0.5, 1]$. Note that the minimum value $h = 0.1066$ of Kolmogorov–Sinai entropy density in that flat regions near $\varepsilon = 0.8$ presents a valley where the system characterizes weak chaotic behaviors. When $\varepsilon \in (0.2, 0.5)$ and $\mu > 3.63$, a valley at $\mu = 3.77$ and $\varepsilon = 0.3$ in the flat regions exists with the minimum Kolmogorov–Sinai entropy density value $h = 0.156$. When $\varepsilon \in (0, 0.2)$ and $\mu > 3.63$, the minimum entropy value in the flat regions is $h = 0.029$. Additionally, the entropy value is zero when the parameter at either $\varepsilon = 0.5$ and $\mu = 3.74$ or $\varepsilon = 0.2$ and $\mu = 3.74$ which characterizes regular behaviors of the system.

The analysis of Kolmogorov–Sinai entropy universality for different parameter values presents the space chaotic behaviors of the ACLML system, as shown in Fig. 2. Five flat regions of the ACLML system containing 100% lattices in chaotic behaviors are divided by four valleys where $\mu = 3.84$, $\mu = 3.74$, $\mu = 3.63$, and $\varepsilon = 0.2$.

The comparisons between the ACLML and the CML systems in Kolmogorov–Sinai entropy indicate that the ACLML system contains more intensive and extensive chaotic

behaviors. Flat regions of the CML system shown in Fig. 3 when $\mu > 3.63$ presents chaotic behaviors are divided by valleys where $\mu = 3.74$ and $\varepsilon = 0.5$, $\mu = 3.74$ and $\varepsilon = 0.3$. Although the CML system has smaller area of valleys than ACLML, the value of 0.2772 in mean Kolmogorov–Sinai entropy density in flat regions of the ACLML system is greater than the value of 0.2718 in that of the CML system. Therefore, considered the effect of various parameters μ and ε , the phase space in the ACLML system diverges greater than that of the CML system. The Kolmogorov–Sinai entropy universality of the CML system for different parameter values is shown in Fig. 4, which indicates the percentage of lattices in chaos. One hundred percent lattices of the ACLML system in chaotic behaviors takes 57.00% of total parameter pairs of ε and μ , while that of the CML system takes 39.17% of total parameter pairs of ε and μ . Fig. 5 shows that how much percentage of different parameter pairs of μ and ε makes the number of lattices of the ACLML or the CML system in chaos. When the number of lattices in chaos exceeds 51% of total lattices, the ACLML system has more parameter pairs of μ and ε than the CML system has. Therefore, the ACLML system has more candidate parameters of μ and ε to achieve space chaos than the CML system has, which is the new feature that the

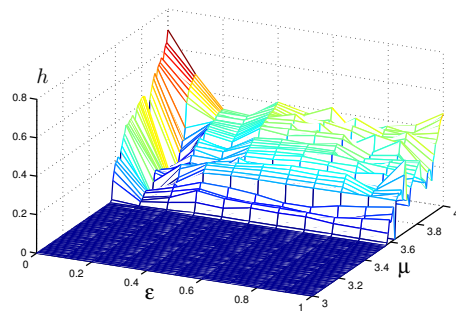


Fig. 1. Kolmogorov–Sinai entropy density for different parameters in ACLML.

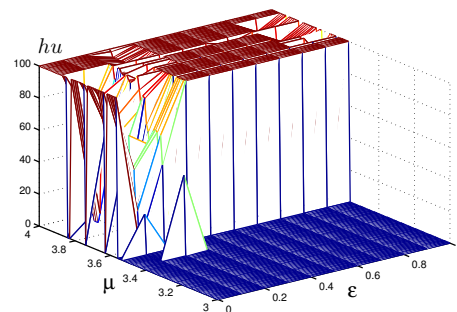


Fig. 2. Kolmogorov–Sinai entropy universality for different parameters in ACLML.

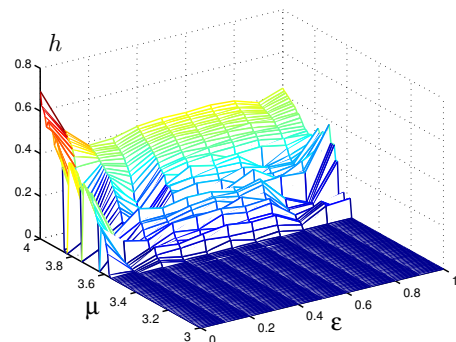


Fig. 3. Kolmogorov–Sinai entropy density for different parameters in CML.

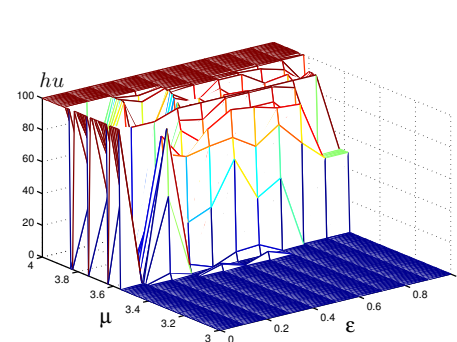


Fig. 4. Kolmogorov–Sinai entropy universality for different parameters in CML.

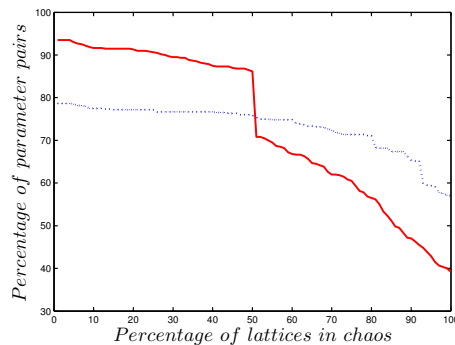


Fig. 5. Percentage of lattices in chaos for different parameter pairs in ACLML (dashed line) and CML (solid line).

parameters of μ and ε can be regarded as the secret keys in cryptography. However, the Fig. 5 also presents that the percentage of total parameter pairs in the ACLML system which is confined to less than 50.00% of total lattices in chaos is less than 80.00% which is lower than that in the CML system. We employ the reactions-diffusions in chemical system for explanation of this phenomenon. The reactions strengthen chaotic behavior and diffusions deduce the effectiveness of reactions. Because of neighborhood coupling in the CML system, diffusions in the CML system can only affect the neighbors in which case the defect and local chaos can easily occur. On the contrary, non-neighborhood coupling in the ACLML system strengthens the diffusions equivalently in which case the energy of this local chaos distributes into other lattices in regular behaviors; therefore, defect and local chaos can not occur in the ACLML system easily.

When the percentage of lattices in chaos exceeds 50.00%, the diffusions in the ACLML system strengthen the chaotic behaviors harder than that in the CML system. Although the amount of energy forces the local chaos in the CML system, the same amount energy in the ACLML system makes majority of lattices approach to their critical points of chaos. Subtle diffusions generate the corresponding interferences which cause majority of lattices in chaotic behaviors.

4.2 Bifurcation in the ACLML system

In both the ACLML system and the CML system, the bifurcation diagrams with $\mu \in [3.5, 3.72]$ in Fig. 6(a) and Fig. 6(b) show the same forking of the possible periods of orbits from 4 to 8. however, such forking of orbits from 8 to 16 in Fig. 6(b) does not exist in Fig. 6(a). The explanation of the difference is that non-neighborhood coupling increases instability of the possible periods of orbits. The non-neighborhood coupling decreases the times of period doubling bifurcations, and the ACLML system becomes chaotic after a point.

There are no periodic windows in the bifurcation diagram with $\mu > 3.70$ for the ACLML system. When chosen some value of parameter ε , the Kolmogorov–Sinai en-

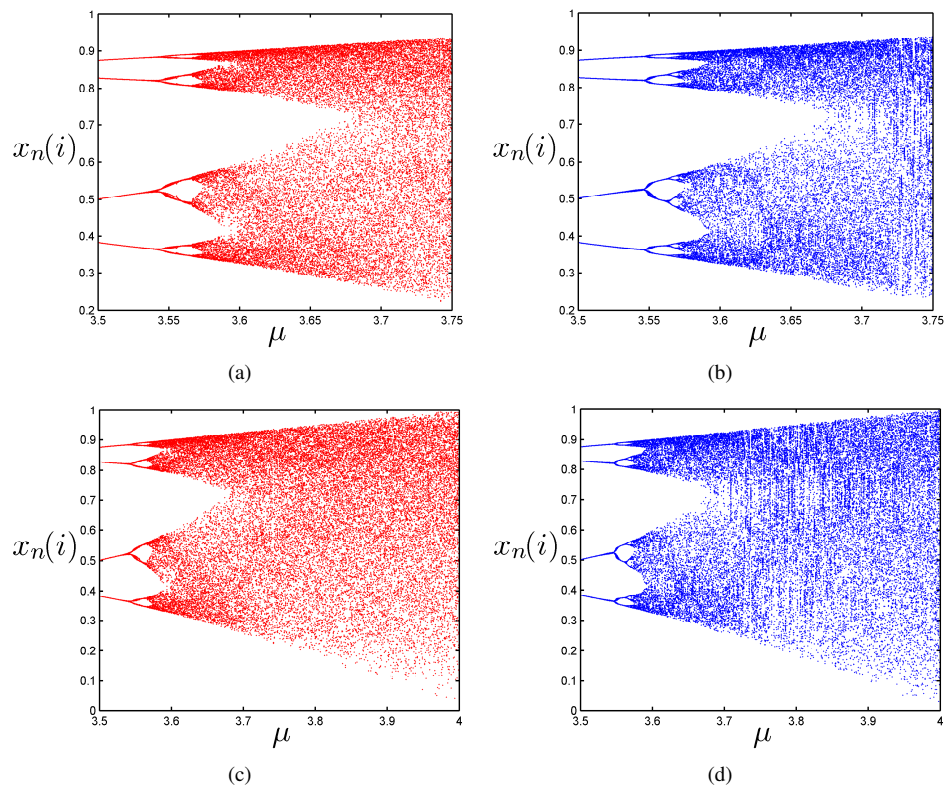


Fig. 6. Bifurcation diagrams: (a) the ACLML system when $\mu \in [3.5, 3.72]$; (b) the CML system when $\mu \in [3.5, 3.72]$; (c) the ACLML system when $\mu \in [3.5, 4.0]$; (d) the CML system when $\mu \in [3.5, 4.0]$.

tropy density is positive in continuously varying parameter μ . And a positive value of Kolmogorov–Sinai entropy density in continuously varying parameter μ is the necessary condition for no periodic windows in the bifurcation diagram. Although positive flat regions occur in the Kolmogorov–Sinai entropy density diagram with a continuously varying parameter μ in the CML system, there are some periodic windows in the bifurcation diagram for the CML system. The entropy density is positive in continuously varying parameter μ in either the CML or the ACLML system when chosen $\varepsilon = 0.3$, which is shown in Fig. 1 and Fig. 2. This phenomenon indicates that non-neighborhood coupling makes the time series distribution wider than neighborhood coupling does. The bifurcation diagrams in the ACLML and the CML systems are shown in Fig. 6(c) and Fig. 6(d), respectively.

The bifurcation diagram without periodic windows in the ACLML system is the new feature for cryptography. The CML system is regarded as a suitable spatiotemporal chaos system for cryptography partially because its less periodic windows than low dimension chaotic map. Thus, the ACLML system is more suitable for cryptography for the same

reason. The parameter μ as secret keys has a larger key space than Logistic map or the CML system. Fig. 5 also implies this new feature hold in most of lattices of the ACLML system.

4.3 Mutual information between lattices

The mutual information value between most of lattices in the ACLML system is zero, which indicates that time series of most lattices in the ACLML system are independent. This feature is suitable for cryptography because the chaotic series in a lattice can not be recovered by other lattices. The mutual information is presented as follows:

$$I(x(i); x(j)) = H(x(i)) - H(x(i) | x(j)),$$

where $x(i) = (x_1(i), x_2(i), x_3(i), \dots, x_n(i))$, $x(j) = (x_1(j), x_2(j), x_3(j), \dots, x_n(j))$ and i, j are the different lattices ($1 \leq i, j \leq L$). We calculate the mutual information in any pairs of lattices in both the ACLML system and the CML system for comparison. Without loss of generality for experiments, we choose $p = 10$, $q = 10$, $\varepsilon = 0.8$ and $\mu = 3.8$ for the ACLML system while we choose $\varepsilon = 0.8$ and $\mu = 3.8$ for the CML system. Fig. 7 shows that the values of mutual information between lattices in the ACLML system are nearly zero because nonlinear chaotic map coupling makes mutual independence of time series of lattices. The only five (i, j) pairs of lattices are $(55, 5)$, $(65, 15)$, $(75, 25)$, $(85, 35)$, $(95, 45)$, and the corresponding mutual information values are 0.853, 0.841, 0.846, 0.858, 0.862. The number of five pairs depends on the size of L lattices. There are 10 lattices of the difference between each pair. When the high values of the pair of $(95, 45)$ plus 10 lattices, the result of $(55, 5)$ is obtained after modulo L ($L = 100$) operation. However, Fig. 8 shows that most values of mutual information between lattices in the CML system are larger than that in the ACLML system. The larger mutual information in the CML system indicates mutual dependence of time series in adjacent lattices for neighborhood coupling. Fig. 9 shows that 99.90% of pairs between lattices with the value of zero in mutual information in the ACLML system, the number of which is greater than that in the CML system of 57.24%. The mutual independence in of time series of lattices in the ACLML system can enhance the security of chaos applications in cryptography.

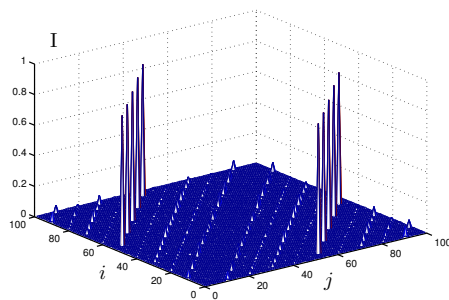


Fig. 7. Mutual information between lattices in ACLML.

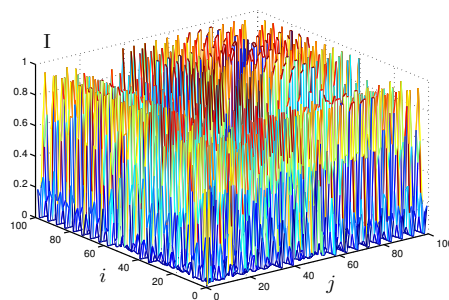


Fig. 8. Mutual information between lattices in CML.

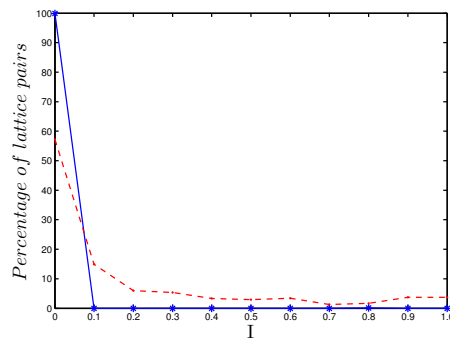


Fig. 9. Percentage of pairs between lattices for mutual information distributions in ACLML (solid line) and CML (dashed line).

4.4 ACLML system behaviors

Because of chaotic map coupling, the ACLML system has fewer patterns than the CML system has. Non-neighborhood coupling strengthens the diffusions between lattices harder than neighborhood coupling does. When majority of lattices in regular behaviors, the chaotic defect of a lattice is difficult to occur because the energy of this candidate lattice in chaotic defect exhaust easily by non-neighborhood coupling. On the contrary, when majority of lattices in the critical points of chaotic behaviors, a subtle defect in a lattice is able to cause the fully chaotic behaviors in all lattices by non-neighborhood coupling. Kaneko [8] discovered the CML system with six patterns. However, the ACLML system characterizes three patterns assumed that the parameter ε is between 0 and 1, μ is between 3.3 and 4.0. The three patterns are listed as follows:

1. *Frozen random pattern.* For situations when $3.3 < \mu < 3.6$ and all values of ε , the ACLML system behavior is regular in which period-2, period-4 and period-8 responses occur. Fig. 10 shows the ACLML system in period-doubling behaviors. When $\mu \in [3.6, 3.7)$ and all values of ε , the ACLML system presents 2I regions of chaos, which is showed in Fig. 11. The random initial value only affects the position of the plot of pattern, which is showed in Fig. 12. This pattern is similar to the CML system in its frozen random pattern except for systems entering 2I regions of chaos. Fig. 13 shows 2I regions of chaos in the CML system. Although Arnold cat map increases the diffusions of spatiotemporal dynamics, the simple regular response in each lattice can not generate complex system behavior.

2. *Pattern competition intermittency.* For situations when $\mu \in [3.7, 3.8)$ and all values of ε , $\mu = 3.8$ and $\varepsilon \leq 0.5$, the system behavior is instable. When increase the value of ε , the select pattern of the ACLML system presents diverse random patterns in a large scale space. Between patterns, the intermittency chaos occurs. Fig. 14(a) shows space amplitude plot of pattern competition intermittency of the ACLML system. When the parameter ε is increased, the patterns in intermittency of the ACLML system may have a larger scale of space showed in Fig. 14(b).

3. *Fully developed turbulence.* For situations when $\mu = 3.8$ and $\varepsilon > 0.5$, $\mu \in (3.8, 4.0]$ and all values of ε , it is difficult to observe any stable behaviors showed in Fig. 15. The reactions dominate the system behavior. The diffusions can not hold the system stable because most of lattices are in chaos and turbulence.

The patterns of defect chaotic diffusion and defect turbulence in the CML system, which are showed in corresponding Fig. 16(a) and Fig. 16(b), are not appeared in the ACLML system because Arnold cat map increases the diffusions of spatiotemporal dynamics. The diffusions dilute the defect which is the local chaotic behavior between neighbor lattices. This dilution by Arnold cat map in non-neighborhood makes the energy in the defect of a lattice exhaust rapidly into other faraway lattices where majority of lattices are in regular behaviors. The comparisons of space-time diagrams between the ACLML system and the CML system, which are showed in corresponding Fig. 17 and Fig. 18, indicate that defect chaotic diffusion pattern and defect turbulence are not emerged in ACLML system. In the defect chaotic diffusion pattern showed in Fig. 17(a), a defect is free-walking in space-time and vanished when tow defects meet.

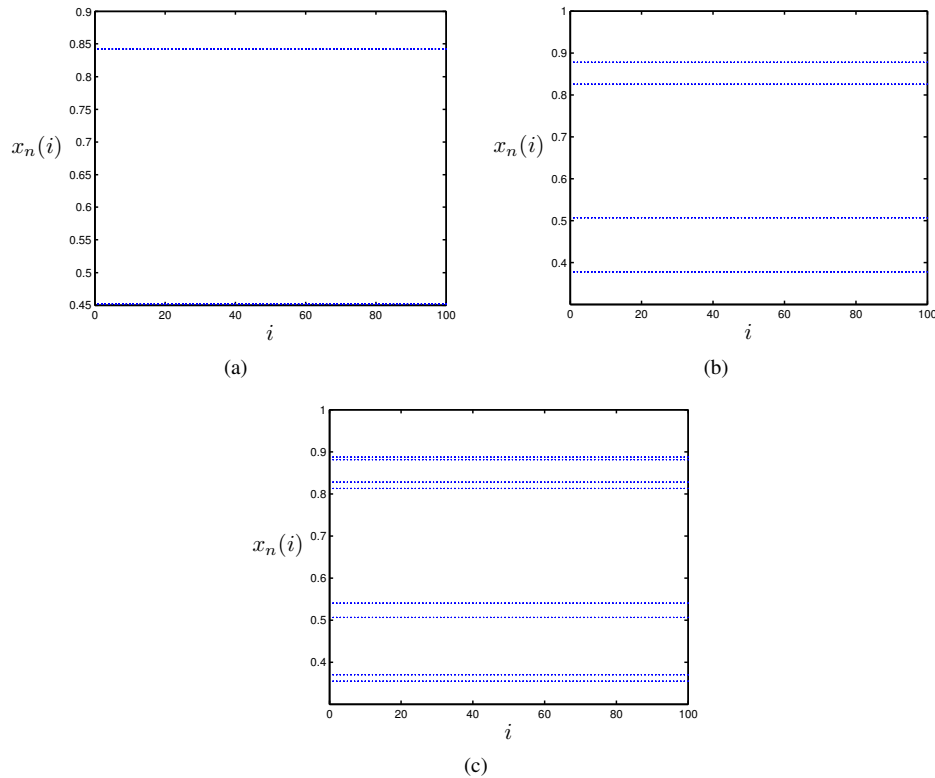


Fig. 10. Regular behaviors of the ACLML system: (a) period-2, ($\mu = 3.4$ and $\varepsilon = 0.5$); (b) period-4, ($\mu = 3.51$ and $\varepsilon = 0.5$); (c) period-8, ($\mu = 3.55$ and $\varepsilon = 0.5$).

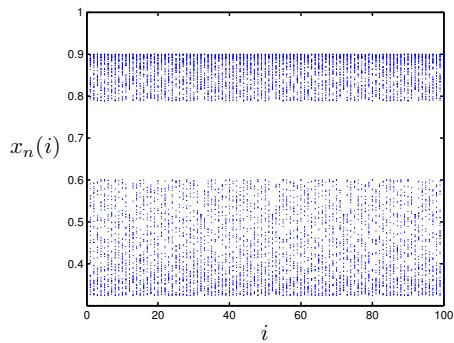


Fig. 11. 2I chaotic regions of the ACLML system ($\mu = 3.6$ and $\varepsilon = 0.3$).

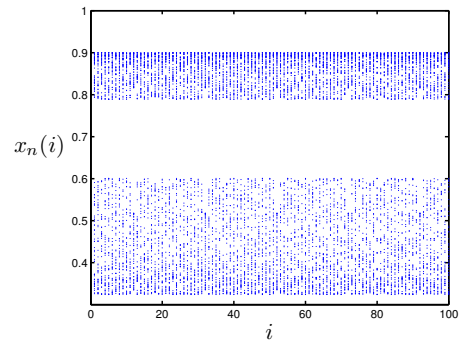


Fig. 12. The random initial value influence of the ACLML system ($\mu = 3.6$ and $\varepsilon = 0.3$).

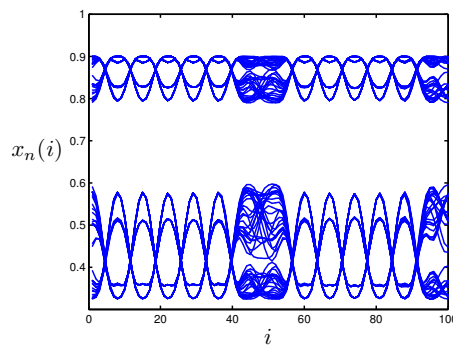
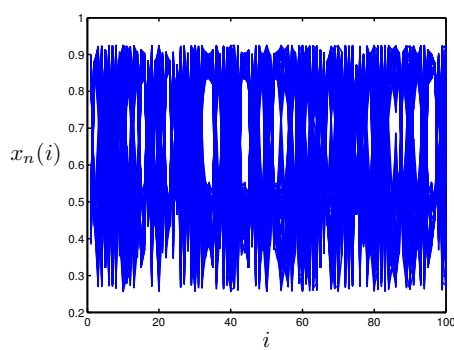
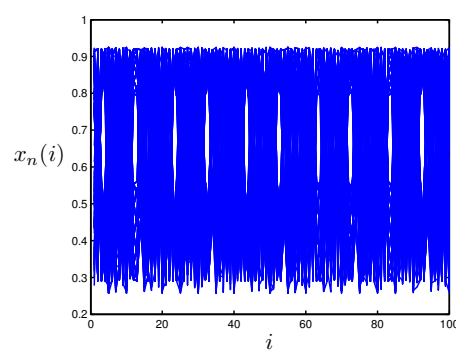


Fig. 13. 2I chaotic regions of the CML system ($\mu = 3.6$ and $\varepsilon = 0.3$).



(a)



(b)

Fig. 14. Space amplitude plot of pattern competition intermittency of the ACLML system: (a) $\mu = 3.7$ and $\varepsilon = 0.1$; (b) $\mu = 3.7$ and $\varepsilon = 0.5$.

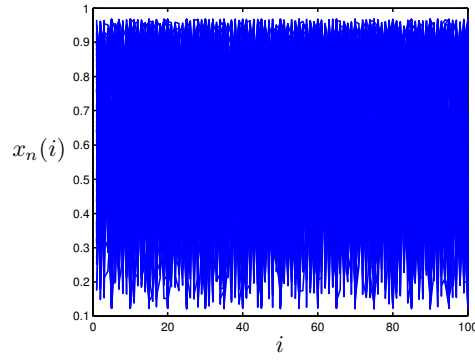


Fig. 15. Fully developed turbulence of the ACLML system ($\mu = 3.87$ and $\varepsilon = 0.2$).

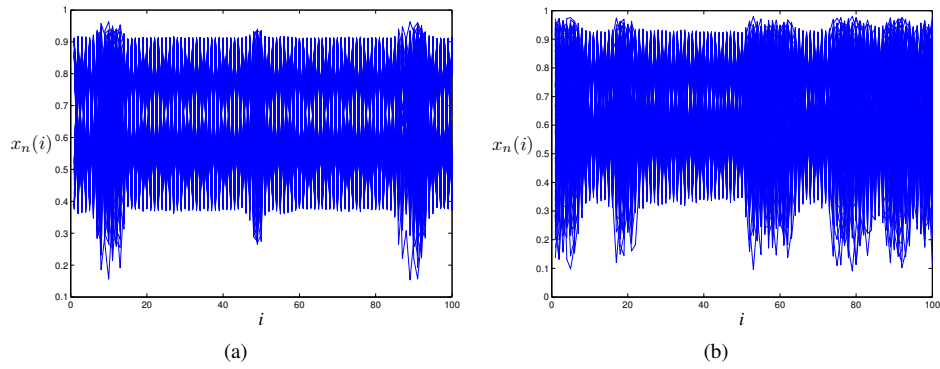


Fig. 16. Defect chaotic diffusion and turbulence of the CML system: (a) $\mu = 3.87$ and $\varepsilon = 0.1$; (b) $\mu = 3.925$ and $\varepsilon = 0.1$.

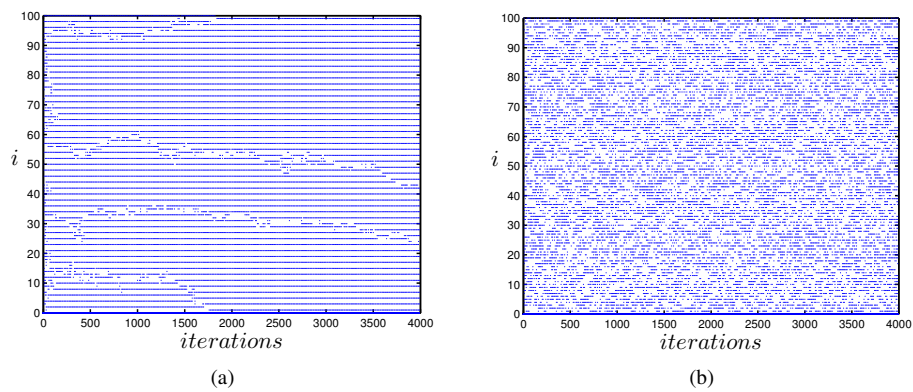


Fig. 17. Space-time diagrams when $\mu = 3.87$ and $\varepsilon = 0.1$: (a) defect chaotic diffusion pattern in the CML; (b) fully developed turbulence of the ACLML system.

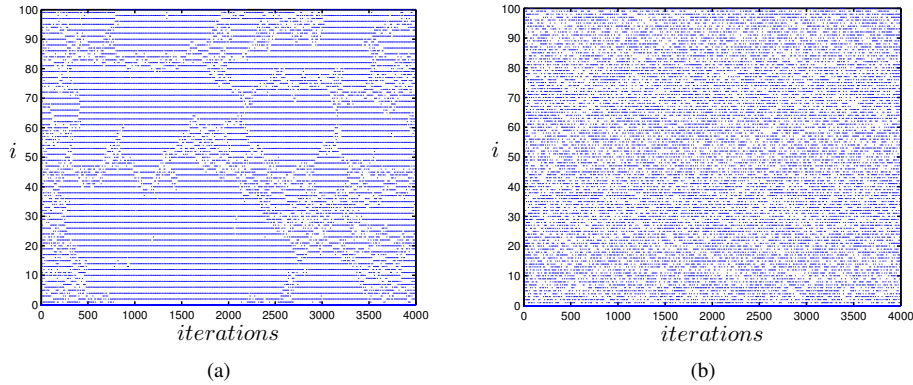


Fig. 18. Space-time diagrams when $\mu = 3.925$ and $\varepsilon = 0.1$: (a) defect turbulence in the CML; (b) fully developed turbulence of the ACLML.

In defect turbulence pattern showed in Fig. 18(a), the number of defects increases when two defects meet. The ACLML system emerges fully developed turbulence pattern showed in Fig. 17(b) and Fig. 18(b) when the CML system emerges defect chaotic diffusion pattern or defect turbulence with the same parameters.

5 Conclusions

This paper deals with the spatiotemporal dynamics of Arnold coupled logistic map lattice. The Kolmogorov–Sinai entropy and space-amplitude diagrams and space-time diagrams are employed to quantify the complexity of system behaviors in the CML system and the ACLML system. The percentage of parameters in the ACLML system of chaos is higher than that in the CML system. This paper also presents that the mutual information of the ACLML system is smaller than that of the CML system. Bifurcations and spatiotemporal dynamics in both the CML system and the ACLML system are also developed in this paper. We obtain the new features such as the lower mutual information between lattices, larger range of parameters for chaotic behaviors, the higher percentage of lattices in chaotic behaviors for most of parameters and less periodic window in bifurcation diagram of the proposed ACLML system. These features are the new properties of the spatiotemporal chaos in form of nonlinear chaotic map coupling method. These features are also suitable for cryptography.

References

1. S. Banerjee, A.P. Misra, L. Rondoni, Spatiotemporal evolution in a $(2 + 1)$ -dimensional chemotaxis model, *Physica A*, **391**:107–112, 2012.
2. D. Cai, D.W. McLaughlin, J. Shatah, Spatiotemporal chaos and effective stochastic dynamics for a near-integrable nonlinear system, *Phys. Lett. A*, **253**:280–286, 1999.

3. Y.H. Chen, J.H. Xiao, Y. Wu, L.X. Li, Y.X. Yang, Optimal windows of rewiring period in randomly coupled chaotic maps, *Phys. Lett. A*, **374**:3185–3189, 2010.
4. C.Q. Dai, R.P. Chen, J.F. Zhang, Analytical spatiotemporal solitons for the generalized $(3 + 1)$ -dimensional Gross–Pitaevskii equation with an external harmonic trap, *Chaos Solitons Fractals*, **44**:862–870, 2011.
5. R. Henda, K. Alhumaizi, Spatiotemporal patterns in a two-dimensional reaction-diffusion-convection system: Effect of transport parameters, *Math. Comput. Modelling*, **36**:1361–1373, 2002.
6. Z. Jabeen, N. Gupte, The dynamical origin of the universality classes of spatiotemporal intermittency, *Phys. Lett. A*, **374**:4488–4495, 2010.
7. Z. Jabeen, S. Sinha, Nonuniversal dependence of spatiotemporal regularity on randomness in coupling connections, *Phys. Rev. E*, **78**, 066120, 6 pp., 2008.
8. K. Kaneko, Pattern dynamics in spatiotemporal chaos, *Physica D*, **34**:1–41, 1989.
9. K. Kaneko, *Theory and Application of Coupled Map Lattices*, John Wiley & Sons, New York, 1993.
10. F. Khellat, A. Ghaderi, N. Vasegh, Li–Yorke chaos and synchronous chaos in a globally nonlocal coupled map lattice, *Chaos Solitons Fractals*, **44**:934–939, 2011.
11. S. Meherzi, S. Marcos, S. Belghith, A new spatiotemporal chaotic system with advantageous synchronization and unpredictability features, in: *Proceedings of the International Symposium on Nonlinear Theory and its Applications (NOLTA'06)*, Bologna, Italy, 11–14 September 2006, Research Society of Nonlinear Theory and its Applications, 2006, 4 pp.
12. A. Mondal, S. Sinha, J. Kurths, Rapidly switched random links enhance spatiotemporal regularity, *Phys. Rev. E*, **78**, 066209, 5 pp., 2008.
13. S. Poria, M.D. Shrimali, S. Sinha, Enhancement of spatiotemporal regularity in an optimal window of random coupling, *Phys. Rev. E*, **78**, 035201, 4 pp., 2008.
14. S. Rajesh, Sudeshna Sinha, Somdata Sinha, Synchronization in coupled cells with activator-inhibitor pathways, *Phys. Rev. E*, **75**, 011906, 11 pp., 2007.
15. S. Sinha, Random coupling of chaotic maps leads to spatiotemporal synchronization, *Phys. Rev. E*, **66**, 016209, 6 pp., 2002.
16. X.F. Zhang, L. Wen, X.B. Luo, Z.W. Xie, Exact solutions of the generalized nonlinear Schrödinger equation with time- and space-modulated coefficients, *Phys. Lett. A*, **376**:465–468, 2012.
17. A. Morozov, B.L. Li, On the importance of dimensionality of space in models of space-mediated population persistence, *Theor. Popul. Biol.*, **71**:278–289, 2007.
18. R. Matthews, On the derivation of a chaotic encryption algorithm, *Cryptologia*, **13**:29–42, 1989.
19. N.K. Pareek, V.K. Patidar, K. Sud, Image encryption using chaotic logistic map, *Image Vision Comput.*, **24**:926–934, 2006.

20. H. Gao, Y. Zhang, S. Liang, D. Li, A new chaotic algorithm for image encryption, *Chaos Solitons Fractals*, **29**:393–399, 2006.
21. J. Fridrich, Symmetric ciphers based on two dimensional chaotic maps, *Int. J. Bifurcation Chaos Appl. Sci. Eng.*, **9**:1259–1284, 1998.
22. A. Akhshani, S. Behnia, A. Akhavan, H.A. Hassan, Z. Hassan, A novel scheme for image encryption based on 2D piecewise chaotic maps, *Opt. Commun.*, **283**:3259–3266, 2010.
23. X. Ge, F.L. Liu, W. Wang, Cryptanalysis of a spatiotemporal chaotic image/video crypton system and its improved version, *Phys. Lett. A*, **375**:908–913, 2011.
24. S.G. Lian, Efficient image or video encryption based on spatiotemporal chaos system, *Chaos Solitons Fractals*, **40**:2509–2519, 2009.
25. S. Mazloom, M.A. Eftekhari-Moghadam, Color image encryption based on coupled nonlinear chaotic map, *Chaos Solitons Fractals*, **42**:1745–1754, 2009.
26. R. Rhouma, S. Belghith, Cryptanalysis of a spatiotemporal chaotic cryptosystem, *Chaos Solitons Fractals*, **41**:1718–1722, 2009.
27. R. Rhouma, S. Meherzi, S. Belghith, OCML-based colour image encryption, *Chaos Solitons Fractals*, **40**:309–318, 2009.
28. S. Wang, W. Liu, H. Lu, Periodicity of chaotic trajectories in realizations of finite computer precisions and its implication in chaos communications, *Int. J. Mod. Phys. B*, **18**:2617–2622, 2005.
29. P. Li, Z. Li, W.A. Halang, G. Chen, A multiple pseudorandom-bit generator based on a spatiotemporal chaotic map, *Phys. Lett. A*, **349**:467–473, 2006.
30. K. Kaneko, Velocity dependent Lyapunov exponent as a measure of chaos for open flows, *Phys. Lett. A*, **119**:397–402, 1987.
31. K. Kaneko, Towards thermodynamics of spatiotemporal chaos, *Prog. Theor. Phys., Suppl.*, **99**:263–287, 1989.
32. H. Shibata, KS entropy and mean Lyapunov exponent for coupled map lattices, *Physica A*, **292**:182–192, 2001.
33. F.H. Willeboordse, K. Kaneko, Bifurcations and spatial chaos in an open flow model, *Phys. Rev. Lett.*, **73**:533–536, 1994.
34. R.M. May, Simple mathematical models with very complicated dynamics, *Nature*, **261**:459–467, 1976.
35. G. Chen, Y. Mao, C. Chui, A symmetric image encryption scheme based on 3D chaotic cat maps, *Chaos Solitons Fractals*, **21**:749–761, 2004.
36. A.V. Holden, H. Zhang, Lyapunov exponent spectrum for a generalized coupled map lattice, *Chaos Solitons Fractals*, **2**:155–164, 1992.